Optical-Model Analysis of the $^{32}S(\alpha,\alpha)^{32}S$ Elastic Scattering from 10.0 to 17.5 MeV†

J. P. ALDRIDGE, G. E. CRAWFORD*, AND R. H. DAVIS
Department of Physics, Florida State University, Tallahassee, Florida
(Received 23 August 1967)

Angular distributions for the elastic scattering of α particles by ^{32}S measured at 100-keV intervals in the bombarding energy range from 10.0 to 17.5 MeV have been analyzed using a two-parameter optical-model description. Real and imaginary potential-well-depth parameters obtained from this analysis oscillate about their respective mean values as the energy is varied. These mean values are interpreted as the potential parameters uncorrected for compound-system resonance effects. Three phase-equivalent real well depths are determined in the analysis: 103, 132, and 163 MeV. The observed rapid variation of the parameters with energy is consistent with a model proposed by Robson, in which compound-system resonances produce an oscillation of optical-model well-depth parameters about mean values which determine the complex potential scattering.

I. INTRODUCTION

IN the beam-energy range accessible with tandem accelerators, good resolution differential cross sections for the elastic scattering of α particles by light nuclei typically vary much more rapidly with energy than do theoretical cross sections computed with the nuclear optical model. At these high excitation energies, the level density is expected to be sufficiently large to justify an optical-model analysis, but the determination of parameters which characterize the complex potential part of the scattering is complicated by the observed strong energy dependence of the α-particle differential scattering cross section.

There are two alternative procedures for extracting optical-model parameters from such data. First, excitation curve data may be averaged to suppress compound-system resonance effects. In this case, the optical model should be modified since the computed results are to be compared with averaged data. This modification requires some model assumptions about the relationships between complex potential scattering and the formation of resolvable compound system or intermediate states. Second, it may be assumed that the compound-system resonances result in a rapid variation of the potential parameters as the energy is varied. The optical-model parameters are determined by averaging the parameters obtained from fits to good-resolution data over an energy interval which is large compared with the widths of the sharp structure in the excitation curves.

The second alternative was adopted in this work and only the well depths of the real and imaginary potentials were allowed to vary with energy. These parameters are observed to oscillate about average values which are identified with the well-depth parameter uncorrected for resolvable compound system resonance effects. A constant average real potential and an average imaginary potential which depends linearly on energy are found. The sometimes rapid variation of the potential parameters about their respective average parameter curves is consistent with a model proposed by Robson which relates the properties of compound-system states to energy-dependent optical-model parameters. This is discussed in Sec. III.

A set of angular distributions for the $^{32}S(\alpha,\alpha)^{32}S$ scattering were obtained for this investigation of the systematic behavior of optical-model parameters. These distributions were measured in 5° angular intervals from 25 to 175 over a bombarding energy range from 10.0 to 17.5 MeV with an energy spacing between distributions of 100 keV. The elastic scattering of α particles by ^{32}S has been previously studied by Farwell and Robison[1] at 43 MeV, Boschitz *et al.*[2] from 30–40 MeV, Gregoire and Macq[3] at 23.8 MeV, Corelli *et al.*[4]

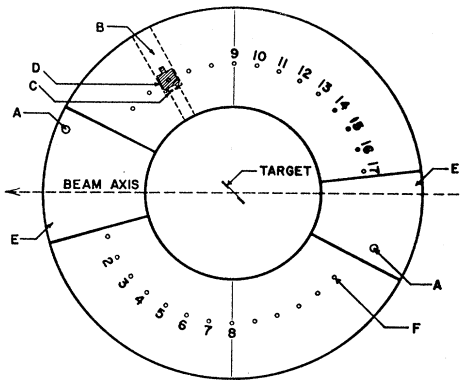

FIG. 1. Schematic diagram of multiple detector array. (A) Alignment pins. (B) Detector slot. (C) Solid angle defining collimator. (D) Silicon surface barrier detector. (E) Slot for beam entrance and exit. (F) Detector retaining screw. The numbers indicate the positions of the detectors used in this experiment.

† Research sponsored in part by the Air Force Office of Scientific Research, Office Aerospace Research, U. S. Air Force, under AFOSR Grant No. AF-AFOSR-440-67. Computing center services supported in part by National Science Foundation Grant No. NSF-GP-5114.
* Present address: Esso Production Research Company, Houston, Tex. 77001.

[1] G. W. Farwell and P. C. Robison, University of Washington Progress Report, 1957 (unpublished). Results quoted by J. S. Blair, Phys. Rev. **115**, 928 (1959).
[2] E. T. Boschitz, J. S. Vincent, R. W. Bercaw, and J. R. Priest, Phys. Rev. Letters **13**, 442 (1966).
[3] G. Gregoire and P. C. Macq, J. Phys. Colloq. **1**, 136 (1966).
[4] J. C. Corelli, E. Bleuler, and D. J. Tendam, Phys. Rev. **116**, 1184 (1959).

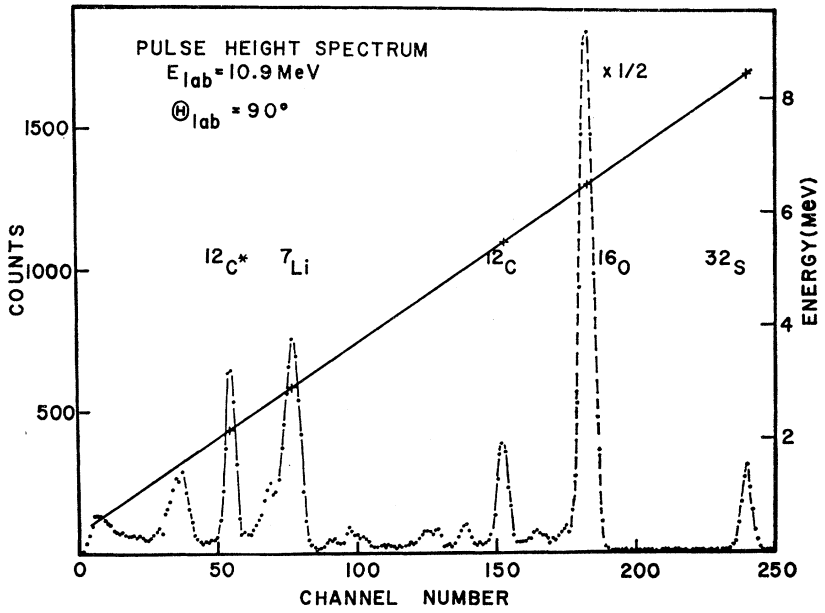

FIG. 2. A typical pulse-height distribution. The line indicates the pulse-height calibration.

at 18.1 MeV, and Hulubei *et al.*[5] at several isolated energies between 12 and 16 MeV.

II. EXPERIMENTAL APPARATUS AND MEASUREMENTS

The He^{++} beam from the Florida State University tandem accelerator was directed onto the target located in the center of an 18-in.-diam scattering chamber.[6] A 120-$\mu g/cm^2$-thick lithium sulfate target evaporated onto a thin carbon backing was used. This target thickness corresponds to an energy loss of about 50 keV for a 10-MeV incident α-particle beam.

Angular distributions were measured using a multiple detector array located on the movable bottom plate of the scattering chamber. Sixteen surface-barrier silicon detectors were mounted in the array (see Fig. 1) at 10° intervals. Rectangular detector collimators, made from 0.20-in.-thick tantalum, afforded an angular resolution of better than ±0.5°. Slit sizes were graduated to keep the counting rates at forward angles comparable to those at more backward angles. With this array, an angular distribution could be measured in 5° intervals with two angular settings of the bottom plate.

Relative solid angles for the detectors were determined by measuring the slit areas of the collimators and the distances from the center of the scattering chamber to the collimators. These measurements were checked by comparing a measurement of the cross section for the elastic scattering of α particles by gold at 10 MeV with the Rutherford scattering cross section.

Pulses from the detectors were amplified using individual preamplifiers and amplifiers for each of the detectors. The amplified pulses were then analyzed using a 4096-channel analyzer, which provided a 256-channel pulse-height spectrum for each of the detectors. A typical pulse-height distribution is shown in Fig. 2. The analyzer also recorded a live time so that correction could be made for counting losses due to analyzer dead time.

The yield in the elastic peak was fed into a computer, which corrected the data for the dead time and solid angle variation and then converted the cross section to the center-of-mass system. The product of this reduction was a printed or punched output of the differential cross section as a function of the center-of-mass angle. A normalization factor for obtaining the absolute cross section was gotten by a comparison of the forward angle ($\theta \leq 90°$) elastic scattering from ^{32}S at 3.3, 4, and 5 MeV to the Rutherford cross section.

An estimated systematic error of 8% is assigned to the absolute cross sections. This consists of a 5% normalization error, a 2% relative solid angle error, and a 1% integrator error. The statistical accuracy was typically about 4%.

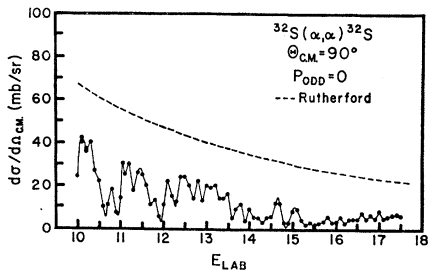

FIG. 3. Excitation curve constructed from the angular distributions. The solid curve connects the data points.

[5] H. Hulubei, G. Semenescu, I. Ivascu, E. Marincu, and R. Dumitrescu, Revue Roumaine Phys., 11, 329 (1966).

[6] E. J. Feldl, P. B. Weiss, and R. H. Davis, Nucl. Instr. Methods 28, 309 (1964).

III. ANALYSIS AND DISCUSSION

Optical-model angular distributions for comparison with the experimental results were calculated using the OPTIX-1[7] code in which the complex potential has the usual Woods-Saxon form

$$V(r)=(U+iW)(1+e^{x})^{-1}+V_c, \qquad (1)$$

where $x=(r-R)/a$ and V_c is the Coulomb potential for a uniformly charged sphere of radius, r_c. The quantities r, R, and a are the radial coordinate, the potential-well radial parameter, and the diffuseness parameter, respectively. This potential is known to possess ambiguities[8,9] which are both discrete and continuous in the parameters. The discrete, or phase-equivalent ambiguities cannot be resolved on the basis of the elastic scattering data alone. This problem has been discussed recently by Thompson *et al.*[9] The continuous ambiguities, such as $UR^2=$const (square well) or

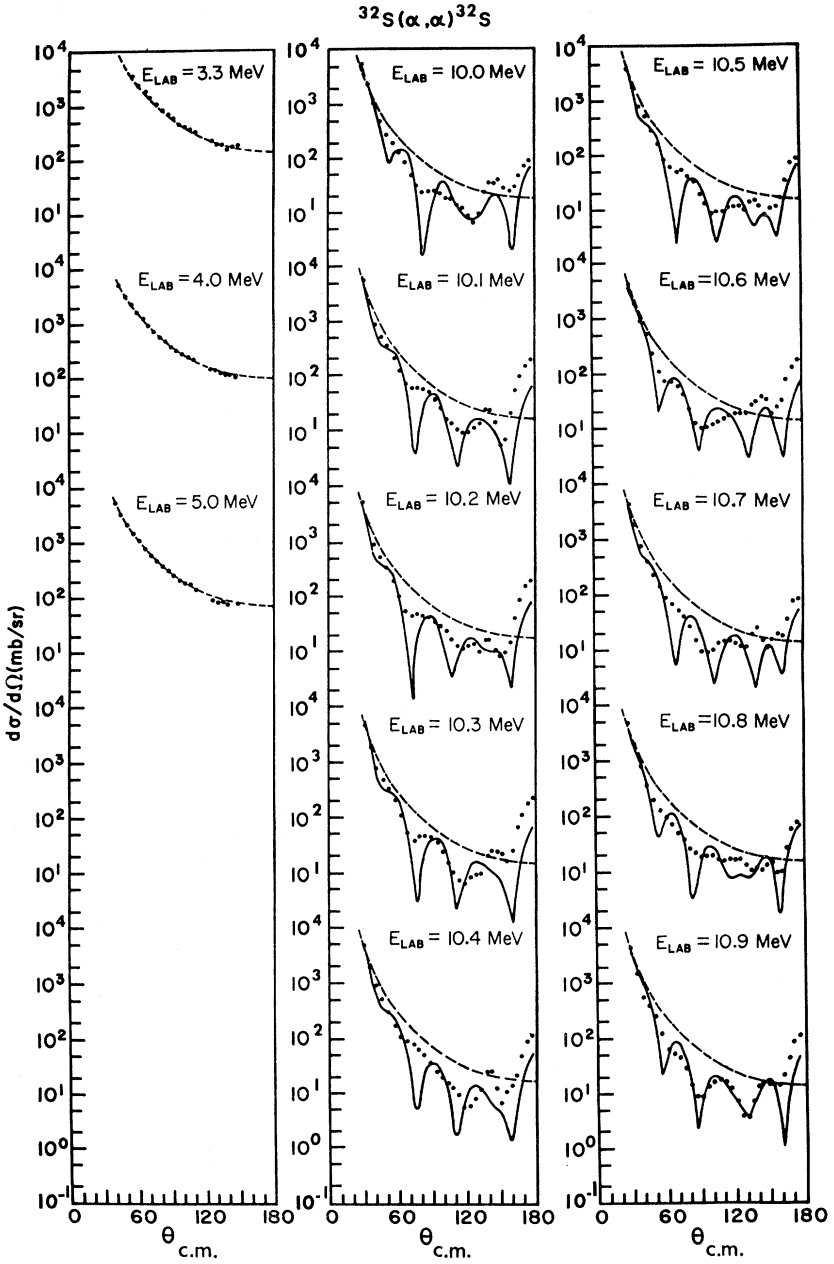

FIG. 4. Angular distributions from 10 to 10.9 MeV. The solid lines are optical-model fits described in the text. The dashed lines are the Rutherford cross sections. The left column shows the low-energy data used for normalization of the cross-section scale.

[7] W. J. Thompson and E. Gille, Tandem Accelerator Laboratory Tech. Rept. No. 9, Florida State University, Tallahassee, Fla., 1965 (unpublished).
[8] R. M. Drisko, G. R. Satchler, and R. H. Bassel, Phys. Letters 5, 347 (1963).
[9] W. J. Thompson, G. E. Crawford, and R. H. Davis, Nucl. Phys. A98, 228 (1967).

$U \exp(R/a) = \text{const}$,[10] mean that the scattering data do not determine the potential strength U independent of the geometrical parameters R and a. Similar remarks apply for W.

The two well-depth parameters U and W were varied to obtain the best optical-model fits to the angular distributions. The best fit criterion was the minimization of the quantity

$$\chi^2 = N^{-1} \sum_{i=1}^{N} \left(\frac{\sigma_{\text{exp}}(\theta_i) - \sigma_{\text{theory}}(\theta_i)}{\Delta\sigma_{\text{exp}}(\theta_i)} \right)^2. \quad (2)$$

The motivation for an optical-model analysis of good resolution data and a subsequent averaging of the parameters is best discussed after examining the energy dependence of the cross section. An excitation curve constructed from the angular distributions is shown in Fig. 3. The observed fine structure cannot be explained with the optical model, but this model should account for the broader underlying structure.

Explanations of similar fine structure as manifestations of intermediate structure or "doorway" states[11]

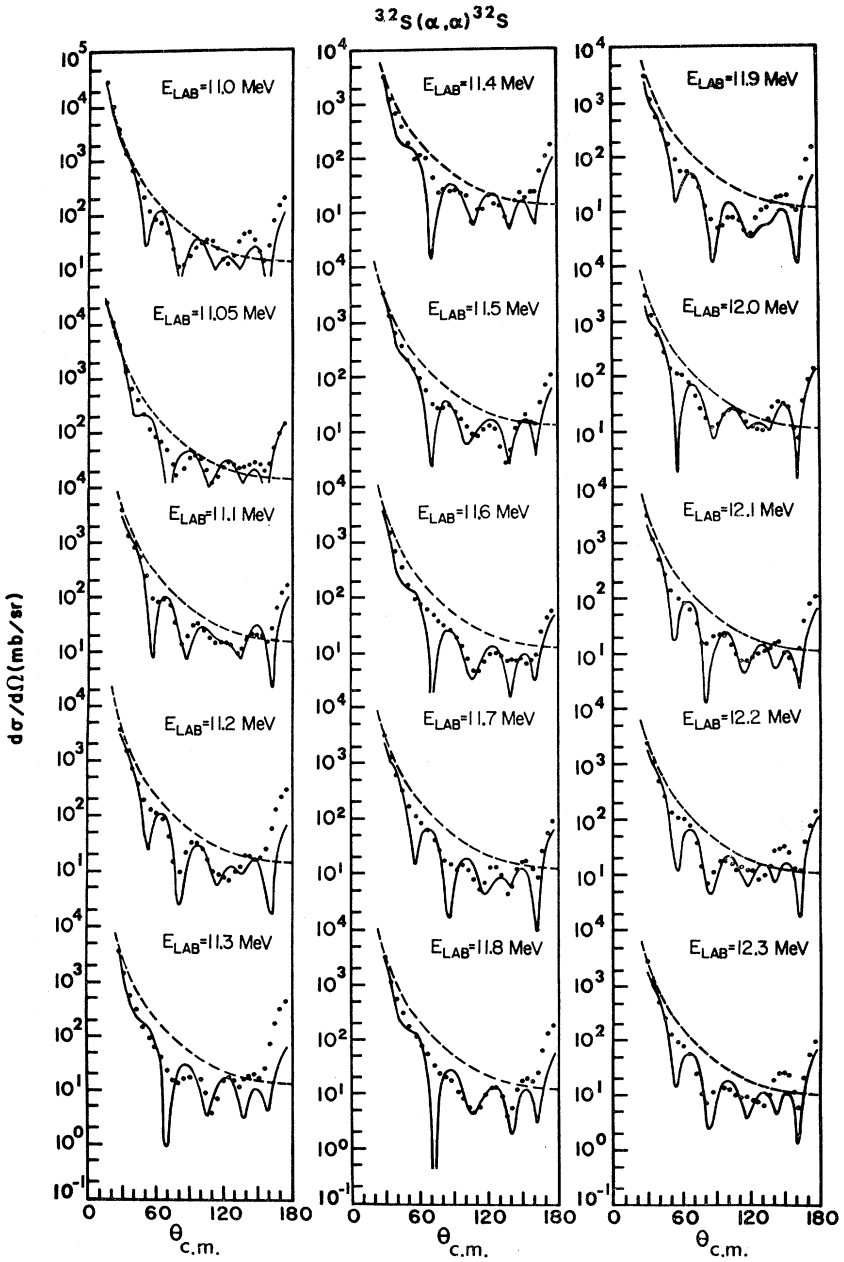

FIG. 5. Angular distributions from 11.0 to 12.3 MeV. The solid curves are optical-model fits. The dashed curves are the Rutherford cross sections.

[10] G. Igo, Phys. Rev. Letters **1**, 72 (1958); Phys. Rev. **115**, 1665 (1959).

[11] H. Feshbach, A. K. Kerman, R. H. Lemmer, *Comptes Rendus du Congrès International de Physique Nucleaire, II*, edited by P. Gungenberger (Centre National de Recherche Scientifique, Paris, 1964).

have been proposed.[12,13] The doorway-state model formulated by Robson[14] is of special interest in the optical-model analysis[12] of good-resolution data since intermediate- or compound-system resonances are introduced as energy-dependent parts of real and imaginary potential-well depths. The real and imaginary potential parameters with one resonance of spin l and width Γ_d at energy E_0 added are given by the expressions

$$U_l=\bar{U}+\frac{\alpha_l^2(E_0-E)}{(E_0-E)^2+\Gamma_d^2/4}, \quad (3)$$

$$W_l=\bar{W}+\frac{\alpha_l^2(\Gamma_d/2)}{(E_0-E)^2+\Gamma_d^2/4}. \quad (4)$$

Thus, as a function of the beam energy, U_l varies symmetrically about a mean potential strength $\bar{U}$, and W_l varies from a mean imaginary potential strength $\bar{W}$. The mean strengths $\bar{U}$ and $\bar{W}$ parameterize a complex potential with no nearby resonance terms added. When several resonances of different spins and parities are present, variations in the potential strengths can be taken to be l-independent. From this model, the average

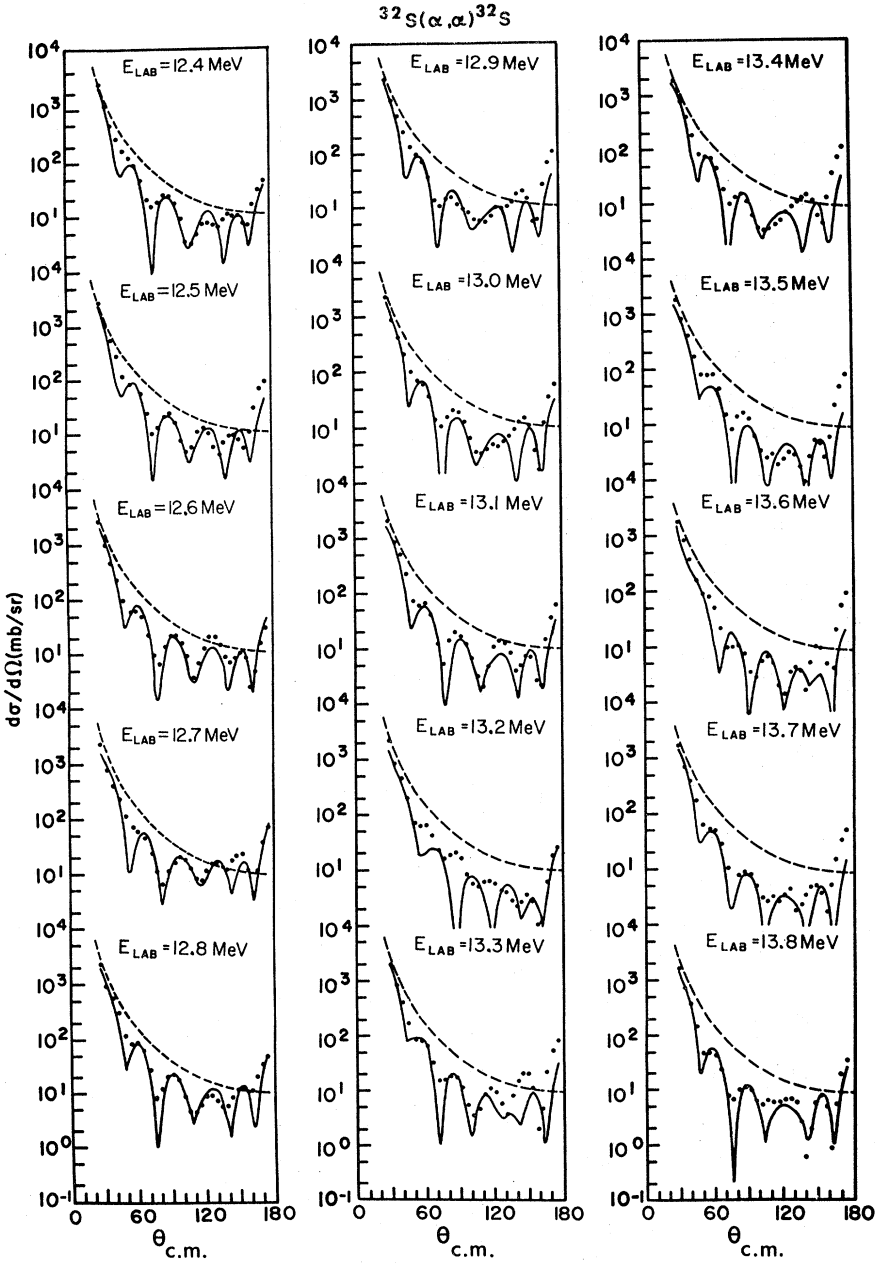

FIG. 6. Angular distributions from 12.4 to 13.8 MeV. The curves are identified in the caption of Fig. 5.

[12] R. H. Davis, *Proceedings of the Symposium on Recent Progress in Nuclear Physics with Tandems*, edited by W. Hering (Max-Planck-Institute for Nuclear Physics, Heidelberg, Germany, 1966).
[13] P. P. Singh, B. A. Watson, J. J. Korepff., and T. P. Marvin, Phys. Rev. Letters **17**, 968 (1966).
[14] D. Robson (private communication).

real parameter $\bar{U}$ is simply determined by averaging measured values of U obtained by fitting good-resolution data. A similar technique is used to estimate $\bar{W}$ although the procedure overestimates this quantity since fluctuation is not symmetric about the mean value. An evaluation of $\bar{U}$ and $\bar{W}$ is a necessary precursor to a more detailed investigation of the fine structure.

The procedure was to compare each angular distribution to an optical-model prediction varying only the potential strengths U and W to obtain the best fit. The geometrical parameters were fixed utilizing the extensive four-parameter search by Lucas, Cosper, and Johnson[15] in the analysis of the 18.1-MeV scattering data.[4] While several sets of significantly different U and W were found in this analysis, the variation of the "best-fit" geometrical parameters was less marked. Their mean geometrical parameter values $R=5.194$ F, $a=0.558$ F and $r_c=3.81$ F, were adopted for use in the present analysis.

The potential strengths were searched in the ranges $90<U<180$ MeV and $0<W<12$ MeV. In these ranges, three sets of phase-equivalent potentials were found as would be expected from square-well con-

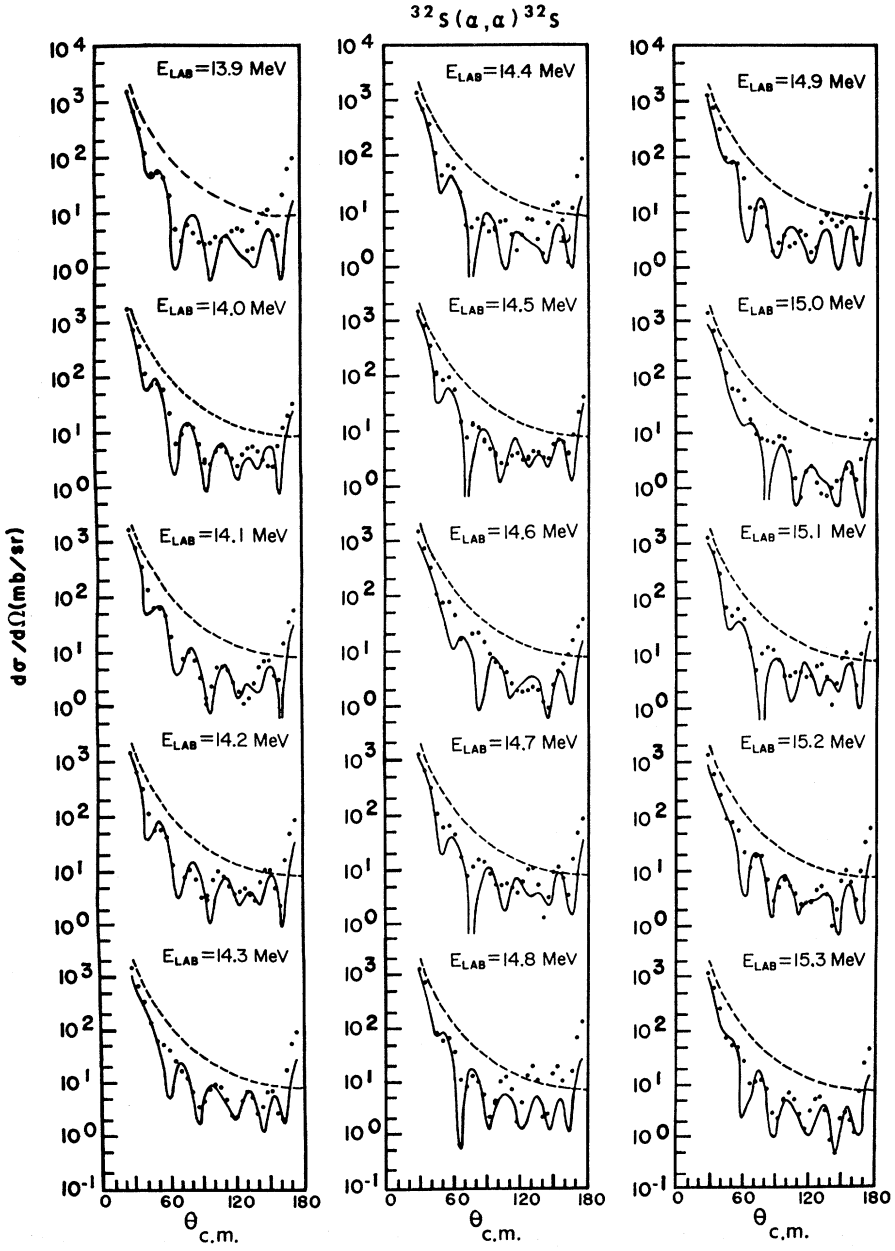

FIG. 7. Angular distributions from 13.9 to 15.3 MeV. The curves are identified in the caption of Fig. 5.

[15] B. T. Lucas, S. W. Cosper, and O. E. Johnson, Phys. Rev. 144, 972 (1966).

siderations.[9] These corresponded to an 8, 9, or 10 node internal s-wave function. The three sets of potentials gave fits to the scattering cross sections of essentially the same quality. The fits for the potentials corresponding to an 8-node wave function are shown in Figs. 4–9.

In general, the features of the experimental data are reproduced. Even for the best fit, the χ^2 value is about 10, indicating that the theoretical calculation falls, on the average, only within about three times the experimental error. Thus the agreement between the optical-model description and the data is only moderately good. A limited variation of the geometrical parameters did not significantly change the quality of the fits.

The nature and significance of the discrepancy between the computed results and the data deserves comment. First, the optical model gives only the shape elastic contribution to the cross section whereas at these bombarding energies the compound elastic contribution is probably not negligible since relatively few channels are open to compete with the elastic channel. Second, the model assumed here, that the fluctuations observed in the excitation curve could be accounted for in terms of variation of two l-independent potential strength parameters is probably too simple. Whereas a more detailed description would undoubtedly produce better fits, systematic features of the few parameters

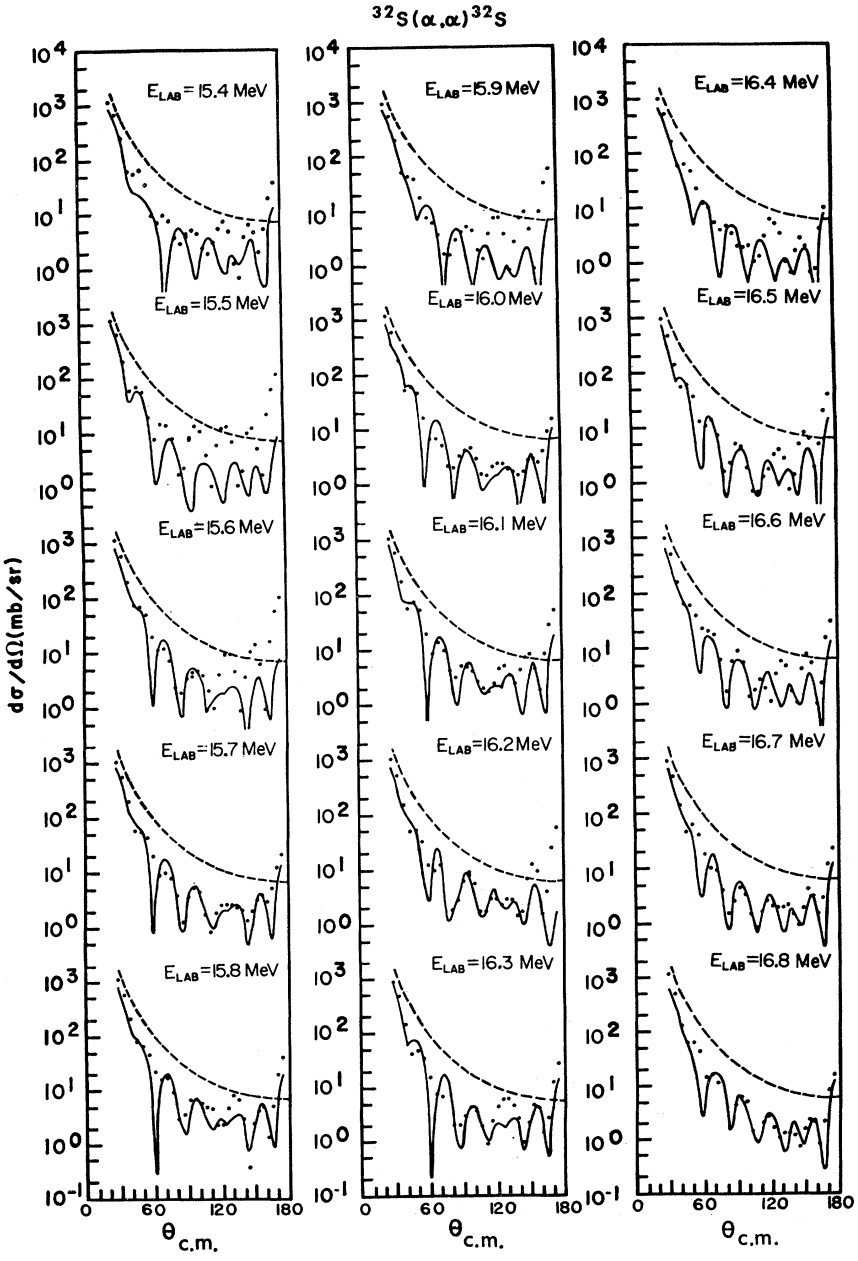

FIG. 8. Angular distributions from 15.4 to 16.8 MeV. The curves are identified in the caption of Fig. 5.

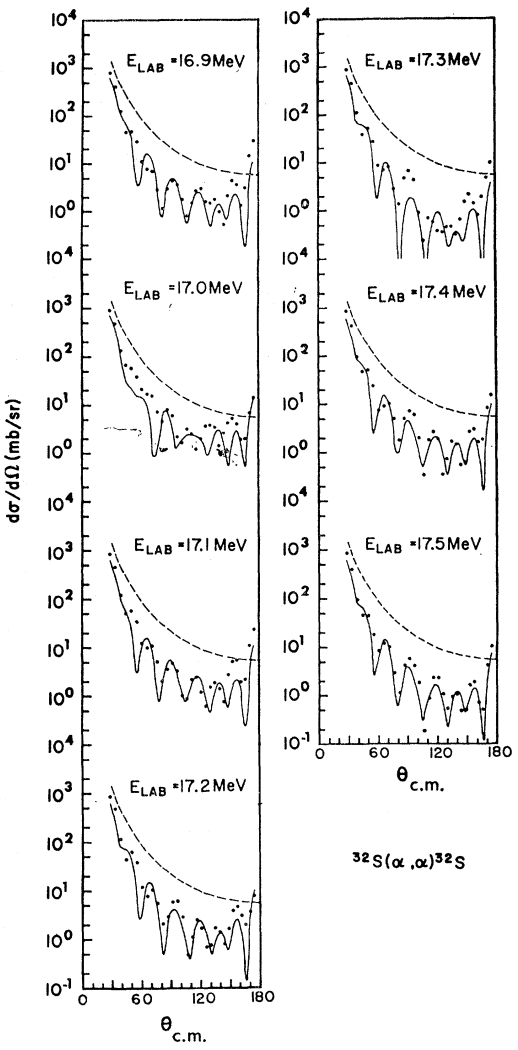

FIG. 9. Angular distributions from 16.9 to 17.5 MeV. The curves are identified in the caption of Fig. 5.

required for the optical-model analysis would be lost in such an analysis. On the other hand, values for the mean optical parameters should not depend sensitively on obtaining detailed fits at each energy.

The best-fit potential strengths for the 8-, 9-, and 10-node wave functions are shown in Fig. 10, plotted as a function of α-particle bombarding energy. Fits from the work of Lucas *et al.*,[15] corrected to their mean geometrical values, which were used here by UR^2 = constant and WR^2 = constant, are shown at 18.1 MeV.

Two features of these curves are noteworthy. First, mean potential strengths are established for each of the phase equivalent solutions by the behavior of the parameters. The mean real strength is constant and the mean imaginary strength rises with increasing bombarding energy. Second, the variations of the potential strengths for the three sets of phase equivalent potentials generally show the same qualitative behavior which is consistent with the assumption that this behavior is due to compound-system resonances and not a spurious effect found in one solution.

While the three sets of potentials produce nearly the same fit, one produces a lowest value of χ^2. At each energy, this potential is indicated in Fig. 10 by a solid symbol. Although the preponderance of best fits for the 8-node wave functions may indicate a preferance for this solution, the possible bias introduced by the choice of the geometric parameters has not been established since extensive searches on these parameters were not performed. Consequently, no conclusion can be drawn from this treatment concerning the proper choice of one potential from among the phase equivalent sets.

The potential strengths obtained were fitted to deduce the mean strengths for the real potential and a linear energy dependence of the imaginary strength. An unweighted fit and a fit to weight the best fits more heavily produces the same results to within 1% for the real strength and 4% for the imaginary strength. The values obtained are summarized in Table I.

TABLE I. Mean potential strengths $\bar{W}=A\,(E_{\rm lab}-E_0)$.

Nodes	Mean $\bar{U}$ (MeV)	A	E_0 (MeV)
8	103	0.89	7.6
9	132	1.00	7.3
10	163	1.14	7.2

IV. CONCLUSIONS

Optical-model fits to the elastic scattering cross section for ^{32}S have been obtained in the energy range from 10 to 17.5 MeV. The mean real potentials associated with the several phase equivalent solutions are constant over this energy range while the mean imaginary potentials rise linearly with energy. The interpretation of broad structure in the excitation function as potential scattering resonances is precluded by the large imaginary potential strengths obtained from the analysis since the smallest observable width would be about 3 MeV. The optical-model potentials obtained here should be useful as a description of the shape elastic scattering underlying the fine structure evident in the excitation function. An investigation of this fine structure is being carried out.

ACKNOWLEDGMENTS

The authors are indebted to Dr. D. Robson and Dr. W. J. Thompson for numerous discussions. The experiment and the analysis were performed with the assistance of A. Bisson, J. Frickey, J. John, P. Robinson, J. Wallace, and B. Watson.

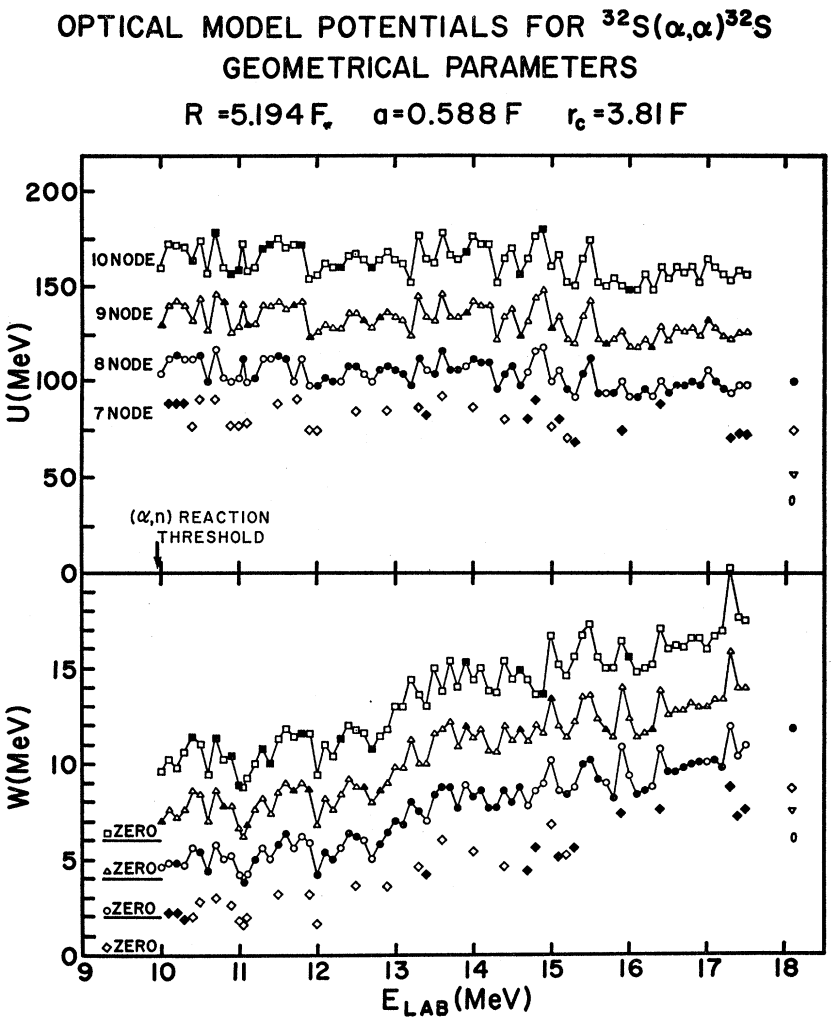

FIG. 10. Best-fit optical potential strengths described in the text. Note the suppressed zeros for W. The potentials adjusted for geometrical differences of Ref. 15 are shown at 18.1 MeV.